# A Simulation Framework for Urban Electric Mobility Based on Limited Widespread Data and Spatial Information

# A simulation framework for urban electric mobility based on limited widespread data and spatial information

Claudia De Vizia, *Student Member, IEEE,* Daniele Salvatore Schiera, *Member, IEEE,* Alberto Macii, *Member, IEEE,* Edoardo Patti, *Member, IEEE* and Lorenzo Bottaccioli, *Member, IEEE*

***Abstract*—Electric Vehicles (EVs) provide an alternative to traditional mobility and a sustainable means of transportation. As a result, electric vehicle sales are increasing across Europe, prompting researchers to wonder about the impact of EVs on smart grids. The proposed framework simulates users' activities, highly characterising individual behaviour using Time Use Survey (TUS) data to estimate EV usage and consumption. Then, for each trip, the routes between origin and destination are determined, simulating in separate modules i) the driving behaviour, ii) the motion of the EV and its discharge considering spatial data and iii) the charge considering users' preference. Thanks to the spatial information openly available, it is possible to characterise the simulation and improve EV consumption estimation. Different scenarios are analysed to demonstrate the versatility of the proposed framework by exploiting its modularity. The individuals' heterogeneity is considered by using an agent-oriented approach. Furthermore, the simulation proceeds on a time-step basis to enable the use of the simulator in a co-simulation environment for future purposes, such as the integration of power networks. The results indicate that achieving a high realism with limited, i.e. containing scarce data for the problem under study, is feasible, enabling researchers to make informed decisions about future mobility.**

***Index Terms*—Electric Vehicles, User activities, Spatial information, Agent-oriented, Time Use Survey, Semi-Markov**

## I. Introduction

The Framework Convention on Climate Change, held in Glasgow in 2021, recognised the need to reduce global carbon dioxide emissions by 45% from 2010 levels by 2030 [1]. Increasing sales of Electric Vehicles (EVs) over the last decade have put Europe on the right track. Furthermore, the European Parliament and Council initially agreed that all new vehicles registered in Europe have to be zero-emission by 2035 [2], i.e. excluding the sale of internal combustion engine cars from that date. This measure might be postponed to a later date [3]. Nevertheless, this decision will eventually boost the diffusion of EVs across Europe. However, the presence of EVs implies additional withdrawal from the grid for recharging or even injections into the grid, considering the innovative Vehicle to Grid technologies, especially in urban areas. Therefore, an accurate estimate of EV usage and consumption is essential for providing effective information for the energy planning and operations of the future energy infrastructure.

Public trials with actual EVs and charging stations can help obtain information, but they have significant costs. Moreover, origin-destination traffic-flow data at any location are not always available [4]. Other possible solutions to estimate EV usage and consumption involve accurate software simulation starting from available data - usually, surveys related to daily activities and transportation patterns. Common approaches for modelling EV usage and short-term interaction with charging stations are based on the activity schedule of individuals, which influences people's travel behaviour [5]. These models shift the emphasis from trips to activities since travels represent a way to connect activities among them.

Several research papers, e.g. [6], [7], attempt to replicate mobility patterns and future EVs behaviours. However, the detail and heterogeneity of the proposed models vary widely. Certain authors, e.g. [8], [9] acknowledge the importance of including socio-demographic (SD), economic and spatial factors and diversifying users' travel patterns. Moreover, few or none consider variable speed, e.g. [4], heterogeneity in the driving behaviour, realistic velocity or road features, e.g. the road slope, which can be included thanks to a spatial dimension, improving our understanding of future mobility.

Almost all reviewed studies, with the exception of [7], use country-specific travel survey data, making the methodology challenging to replicate in other countries as their data are not standardised within a common data framework. The majority of authors used National Travel Statistics data. However, of 29 European countries surveyed in [10], only eight countries make data available. When more accurate data are unavailable, a standardised methodology based on limited widespread data, i.e. non-specific for the problem under study, would be helpful to gain insight into future mobility in Europe.

Consequently, this work aims to provide a practical framework based on limited and openly available data that characterise the different individuals in depth to replicate realistic driving behaviour and corresponding EV consumption, enabling the comparison of plausible scenarios.

The proposed methodology uses Time Use Survey (TUS) data - a large sample survey on places visited, daily activities and travels performed by the residential population - characterising the synthetic population with socio-demographic attributes. It is essential to notice that these national surveys are available in almost all countries and broadly comparable across countries [11]. The data are used to generate daily residential synthetic sequences of activities thanks to the proposed model based on state-of-the-art methodologies, e.g. [12], [13]. A spatial layer that is openly available is considered to simulate plausible and variable road speeds. The model uses road features and driving behaviours to simulate realistic car

trips. Then, the power consumption of the EV is determined by considering vehicle features, too.

To consider the heterogeneous behaviour of people and enable future improvements of the framework, we adopt an agent-oriented approach, thanks to the Python library AIOMAS [14]. AIOMAS is a library for remote procedure calls, request-reply channels, and an agent layer. In AIOMAS, agents can be spawned to parallelise the application and increase the number of agents present in the simulation. Following a modular approach, the user agent implements each user's behaviour, intelligence, and characteristics, while the EV agent is considered a separate agent. Breaking down the framework into smaller modules improves code re-usability, allowing us to update a single module without changing the others and making the framework versatile.

The simulation proceeds on a time-step basis so it can be synchronised and used in a co-simulation environment for future purposes, e.g., performing an in-depth evaluation of the impact of EVs on a given distribution grid.

The remainder of this work is divided into four sections. Section II compares the proposed methodology with the existing literature. Section III presents all modules of the framework. Section IV progressively validates the different modules and then analyses the results for various scenarios considering user behaviours. Finally, Section V draws conclusions and suggests future work.

## II. State of the Art

In this section, the methodologies presented by several authors to simulate future mobility patterns and consumption are summarised in Table I and compared with the proposed solution.

The authors of [7] used UK 2000 TUS survey for generating driving patterns thanks to a nonhomogeneous Markov Chain Monte Carlo simulation. The EV status was classified into driving, parked at home, in commercial areas, and at work. To the best of our knowledge, only [7] used TUS data (see column "Input data" of Table I). However, it did not include a spatial layer. The use of widely available datasets enables the reproducibility of the methodology in several countries.

In [9], the EV usage in a year and the total number of trips based on driver occupation and household type were sampled from the "Mobility in Germany" study, specifically focused on German everyday mobility. They used a nonhomogeneous Markov chain to determine a sequence of destinations for each trip. The locations were abstract, e.g. inside the city, outside the city. They used a second variable to differentiate and characterise trips, e.g. shopping. The distance travelled was sampled from a distribution that considered travel purpose and employment of the driver. Finally, they sampled each day's driving and parking times and the vehicle speed. Starting from the same data, [13] proposed a simplified stochastic model based on a nonhomogenous semi-Markov process considering three states: i) parked at home, ii) parked at work and iii) parked elsewhere. As opposed to [7], the driving action was not modelled as a separate state. Thus, the driving time became part of the sojourn time of the other states. The stochastic process was then extended to consider charging and driving processes. A consumption of 20 kWh/100 km was considered. Also, Shepero et al. [15] used a specific consumption, i.e. 0.25 kWh/km, assuming that the size of the battery is irrelevant. They employed GIS data to extract the location of parking spaces and clustered them by use type, e.g. "home". Then, they used a nonhomogeneous Markov chain to locate the EVs at each step and calculated the charging load at each parking lot. They used the Swedish travel survey, eliminating the driving state. Thus, EVs switched between parking states instantly.

The authors of [6] categorised the travel patterns of drivers into different categories using data from the Finnish national traffic survey. Each travel activity's arrival and departure times were defined through a probability distribution. They calculated the distance and departure time. In [8], the initial time of the first travel was sampled from the corresponding distribution. The destination of a trip was sampled from the spatial transition probability, i.e. home, work and other, considering the time and the place. The trip length and the distance were sampled, and the parking duration was defined. The proposed method was validated using the US National Household Travel Survey data. The same data were used by Xiang et al. [4], who used Monte Carlo sampling method to generate daily destinations starting from the home. A 2-trip or 3-trip chain was established. The parking, charging and driving were examined using the proposed spatial-temporal method.

Torres et al. [17] randomly selected activity patterns from probability tables at the beginning of the day. The authors used Anylogic to model the EV agent. Here, there was no distinction between the user and the vehicle. This distinction would have allowed the behaviour and intelligence of a user and the physical behaviour of a vehicle to be characterised separately, thus having major flexibility. The EV agent's home and workplace were fixed, whereas other activities were computed at runtime. Also in [16], the EV agent combined the EV and the driver behaviour in one entity. The activities of the agents were sequences of 3-5 activities randomly sampled whose duration followed a normal distribution. The location of the activities is selected randomly. Starting from an actual dataset on charging patterns, Wolbertus et al. [18] presented an agent-based model to analyse the consequences of charging choices and charging station deployment. They assumed that charging demand was not directly correlated with travel patterns but rather the result of an interplay between parking and charging needs. The analysis was very interesting; however, it required a considerable amount of data that was not usually available.

Zhang et al. [8] stressed the importance of including demographic and social characteristics in the analysis - an observation also made by the authors of [9], who presented a model capable of generating stochastic, socioeconomically differentiated electric load profiles for EVs. Despite their importance, SD factors were only considered by a few authors, as shown in column "SD" of Table I.

The column "Charging strategies" summarises the different charging strategies tested. The majority of the strategies were related to the parking lot, e.g. "Home" or to the State Of Charge (SOC) of the EV. The aware and unaware users in [16] reflected the SOC level at which an EV agent recharged,

TABLE I: Comparison of the proposed work with the existing literature

| Paper | Input data | Road network | SD factors | Charging strategies | Charging power [kW] | Battery capacity [kWh] | Speed trajectory | Aerodynamic vehicle model |
|---|---|---|---|---|---|---|---|---|
| Wang et al. [7] | UK TUS survey | ✗ | ✗ | When parked at home / work | Fast and normal | 18.8 | Constant (30 mph) | ✗ |
| Rolink et al. [13] | *Mobility in Germany* study | ✗ | ✗ | At home and work | 3.7 | - | ✗ | ✗ |
| Shepero et al. [15] | Swedish Travel Survey | ✗ | ✗ | At home OR everywhere | 3.7, 6.9, 22 | - | ✗ | ✗ |
| Marmaras et al. [16] | UK Energy Research Centre | ✓ | ✗ | Aware OR unaware user | 7.4, 22 | 53 | Constant along a road | ✓ |
| Torres et al. [17] | Probability table with real data | ✓ | ✗ | Always when parked OR if SOC below 20% | 22, 50 | 16.9-60 | ✗ | ✗ |
| Xiang et al. [4] | US National Household Travel Survey | ✓ | ✗ | After driving OR when the demand cannot be met | 7, 30 | 20 | Speed-flow model | ✗ |
| Fischer et al. [9] | *Mobility in Germany* study | ✗ | ✓ | Logistic function to model charging prob. upon SOC | 3.7, 11, 120 | Several | Sampled for each trip | ✗ |
| Zhang et al. [8] | US National Household Travel Survey | ✗ | ✓ | When not enough energy for next trip OR always | 4, 8 | 40 - 50 | ✗ | ✗ |
| Iqbal et al. [6] | Finnish National Traffic Survey | ✗ | ✓ | At anytime OR from 20:00 onward | n.s. | 8.8-24 | Sampled for each trip | ✗ |
| Wolbertus et al. [18] | Dataset on charging patterns (Amsterdam) | - | - | - | 50, 175, 350 | between 4 and 100 | - | - |
| **Proposed solution** | IT TUS survey | ✓ | ✓ | At home OR SOC below 50% | 11 | 40 | Variable | ✓ |

e.g. when necessary or frequently. Columns "Charging power [kW]" and "Battery capacity" list the values usually used.

From the column "Speed trajectory" of Table I, it is possible to notice that [4] used a speed-flow model, modelling different speeds on different road segments. Instead, other authors, e.g. [6], sampled the value of the vehicle's average speed for each trip. Thus, an average speed is assigned to each trip, and different trips during the day have different average speeds. However, there is no variability in speed in a single trip. Instead, "variable" indicates a variation in speed in each road segment and inside the same stretch of road. The majority of the other researchers considered the speed of the vehicles equal to the average speed, i.e. *constant* - a data usually available - or do not consider speed, but an average consumption, e.g. [17]. However, this simplification has a substantial impact on the consumption of the EV. A spatial dimension can be introduced to overcome this problem and introduce variability. Nevertheless, most works have not considered a road network, as noticeable from column "Road network" in Table I. Torres et al. [17] included a spatial dimension preprocessing geographic data using ArcMap, which can include actual traffic flows. However, they then used a very simplified road network. The authors of [4] considered a road network which consists of vertex and connected edges. For the test case, the map included 52 roads. Anyhow, they then used this information to determine the driving time, assuming a constant EV consumption. Marmara et al. [16] modelled interactions in both road transport and electric power systems. A road transport network with ten nodes was considered. They also modelled traffic following a macroscopic approach.

Adding an aerodynamic vehicle model that receives as inputs driving patterns simulated thanks to the information received from the spatial layer makes it possible to improve the simulation. Only [16] included an aerodynamic vehicle model (column "Aerodynamic vehicle model" of Table I). However, the authors considered a constant speed along an avenue. Thus, they omit acceleration.

To the best of our knowledge, regardless of the dataset used, it does not emerge that other authors considered i) a detailed spatial layer containing real data and ii) realistic driving behaviour, which translates into variable speeds on the road, factors that strongly influence EV consumption. Using real information contained in the spatial layer offers many advantages. First, it provides information on speed, which varies greatly in the urban context. In addition, it is possible to determine the slope of the roads, another factor that substantially impacts vehicle consumption that no other author in Table I considers.

Thus, the overall novel contribution of this work can be summarised in:

• a methodology based on widespread data, i.e. TUS survey and openly available spatial data, thus replicable and suitable for different cities and countries. Column "Input data" in Table I highlighted the used dataset. The non-private European datasets (German, Finnish and Swedish surveys) belong to the 8 European countries that make country-specific data available [10]. Since TUS are not travel-specific surveys, the spatial information, e.g. speed on each road and slope, helps improve the simulation with the features of the city under study. The spatial dimension helps generate accurate driving patterns exploitable by the aerodynamic vehicle to enhance the estimation of EV consumption. The heterogeneous characteristics and driving behaviours have been considered thanks to adopting an agent-oriented approach.

• the implementation of a modular framework that allows us to use only a subset of the models and easily add new components to accommodate more complex scenarios, such as the grid. Moreover, the ability to generate the data and proceed on a time-step basis enables us to couple the proposed framework with other simulators in a co-simulation environment, e.g., integrating the power network simulation. Therefore, it is possible to synchronise data with other simulators, use all the necessary data at that time step, and save only the data of interest for the simulation under study.

## III. Methodology

This paper presents a novel framework that simulates daily human behaviour to recreate travel activities and evaluate the impact of EVs with non-specific but widespread data. The framework in Figure 1 can be divided into five main modules: i) the *Activity Pattern*, ii) the *Path Generator* iii) the *Driving Behaviour*, iv) the *Charging Strategy* and v) the *EV model*. The proposed framework implements two types of agents: the *User Agent* and the *EV Agent*. The *Activity Pattern*, the *Driving Behaviour*, and *Charging Strategy* are the core engine of the *User Agent*. The *Path Generator* focuses on the interactions of the user agent with the spatial environment, while the *EV model* is the core engine of the *EV Agent*.

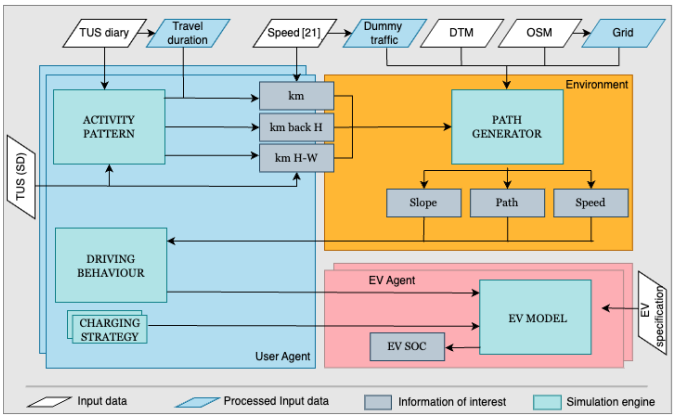


Fig. 1: Schema of the proposed framework

### A. Activity Pattern

Based on the daily 10-minute resolution of the *TUS diary*, the non-travel activities of those who made at least one trip by car during the surveyed day can be identified considering the location where the activity occurred.

As opposed to travel surveys, in TUS, an individual's transition from one activity to another does not always involve a car trip, i.e., the car is still parked at the same location. Therefore, it is necessary to make some assumptions to be able to use TUS data. In particular, it has been assumed that a sequence of non-travel activities in the TUS diary comes down to what is considered the most significant activity, i.e. the main motivation for that trip. For example, a person may go to work by car, walk to a restaurant close to their workplace, and then return to work. In this case, the main motivation for the trip by car would be "Work." The same applies if, for example, the user goes to the pharmacy before entering the workplace —and no car trip is registered in between.

The resulting "priority" associated with the activities is summarised in Table II. The "priority" determines which activity is the main motivation for the trip.

TABLE II: Priority associated to the non-travel activities

| Priority | Activity |
|---|---|
| 1 | Home |
| 2 | Work |
| 3 | Study |
| 4 | Social life and sport |
| 5 | Supermarkets and healthcare |
| 6 | Other |

While most authors consider "Home", "Work", and "Other", in the proposed methodology the activities that are commonly classified as "Other" are better characterised. Indeed, the "Study" activity has been distinguished from the "Other" activities since it is strictly related to a subset of the population. Moreover, in [19], it emerges that the average kilometres travelled for going to the grocery are much less than those travelled to leisure activities. Therefore, "Supermarkets and healthcare" have been distinguished from "Social life and sport".

The type of activity carried out is closely related to the time of day; instead, travels are a way to connect activities. Indeed, the approximate length of the travel in kilometres does not depend on the time of day but on space, that is, the geographic location of the next activity. Similarly to [13], travels are not modelled as separate states. Thus, the time considered for the travel activities is incorporated with the significant activity following the travel, resulting in an increment in the duration of the non-travel activity.

The socio-demographic characteristics of the users interviewed selected in this analysis are the gender and the employment status, i.e. *full-time worker*, *part-time worker*, *student*, *fulfilling domestic tasks*, i.e. housewife/househusband, and *unemployed/pensioner*. As it is possible to notice from the *TUS (SD)* block in Figure 1), this distinction is considered in the *Activity Pattern* block, i.e. for the creation of the transition matrices as explained in the following, and the commuting distance, which is sampled based on the user gender and profession.

Based on the simulation's set-up, a certain number of user agents characterised by the SD parameters considered in the input data can be created. Moreover, each user agent is assigned the house coordinates. Depending on the scenario, the selection of house coordinates can reflect the building density of residential areas or be random. The workplace is selected considering the distance declared in the TUS between home and work.

People's daily behaviour can be seen as a sequence of activities that can be modelled through stochastic methods. As can be observed by the review of existing literature in Section II, nonhomogenous Markov chain [20] can be used to generate the activity pattern since the probability of performing certain activities, e.g. "Work", varies throughout the day. However, other authors chose a nonhomogenous semi-Markov

chain, e.g. [12] [13]. Indeed, the semi-Markov process is a generalisation of the Markov process since, as underlined by [13], semi-Markov processes allow for an arbitrarily distributed sojourn time, overcoming the limitation of the Markov process where the sojourn time is exponentially distributed.

Thus, on a complete probability space, the two following random variables are defined:

i) $X_n$: $\Omega \rightarrow$ E, which represents the state at the $n^{th}$ transition

ii) $T_n$: $\Omega \rightarrow \mathbb{N}$, which is the chronological time of the $n^{th}$ transition.

Let E = {Home, Work, Study, Social life and sport, Supermarkets and healthcare, Other}, i.e. the activities in Table II, be the state space. The associated non-homogeneous semi-Markov kernel Q is

$$\begin{aligned} Q &= [Q_{i,j}(s,t)] \\ &= [P(X_{n+1} = j, T_{n+1} \leq t | X_n = i, T_n = s)] \end{aligned} \tag{1}$$

*i,j* $\in$ E, *t,s* $\in \mathbb{N}$.

The transition probabilities and sojourn distributions must be computed to generate a new activity sequence. Thus, from TUS data, 144 6x6 transition matrices are created, i.e. one every 10 minutes, for each user type - gender and profession - and both weekdays and weekends. Each element $p_{ij}(s)$ of a matrix, i.e. the probability of going from state I to state j (*i,j* $\in$ E), is computed as

$$p_{ij}(s) = \frac{a_{ij}(s)}{\sum_{k=1}^{6} a_{ik}(s)} \tag{2}$$

where $a_{ij}$ is the number of transitions observed in TUS data from state i at time s to state j. Moreover, the sojourn time unconditional and conditional cumulative distributions are defined respectively as:

$$F_i(s,t) = [P(T_{n+1} \leq t | X_n = i, T_n = s] \tag{3}$$

$$F_{ij}(s,t) = [P(T_{n+1} \leq t | X_n = i, J_{n+1} = j, T_n = s] \tag{4}$$

Again, the sojourn time can be computed from the raw data as described in [21]. After computing the transition probabilities and sojourn distributions, it is possible to generate the activity patterns with Monte Carlo algorithm, obtaining the sequence of visited states, i.e. non-travel activities, and jump times as done in [22] and in [12].

### B. Path Generator

The generated sequence of activities does not explicitly include travels. The proposed methodology considers a spatial layer to determine them by introducing the *Path Generator*, as depicted in Figure 1.

To create the spatial layer, road network data can be downloaded from OpenStreetMap (*OSM*) [23]. The road network also contains other important information, such as the speed limit. The map can be viewed as a graph where the intersections of the roads, i.e. the edges, are the vertices or nodes. Thus, the graph containing all the information can then be accessed to find the shortest path between two nodes, i.e. the travel performed by the agent.

Moreover, thanks to the Digital Terrain Model (*DTM*) - i.e. a representation of the earth's surface elevation excluding the vegetation and the anthropic elements - it is possible to retrieve the earth's surface heights in each location. Therefore, for each map segment, i.e. road length and altitude difference, it is possible to know the road slope. If this information is unavailable, the slope can be set to zero without affecting the rest of the framework.

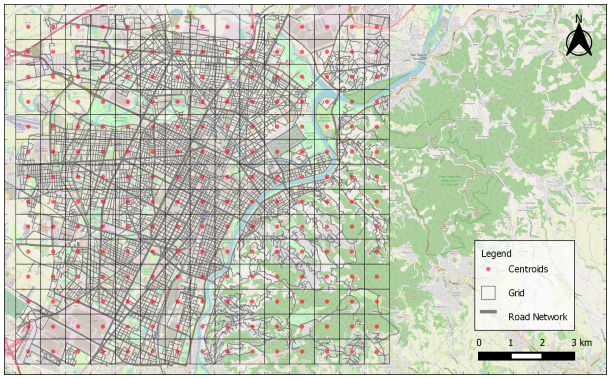


Fig. 2: Centroids for a grid of approximately 1km square

While activities are determined using a stochastic model to determine the travel activity, the behaviour and movement of the users are also considered. Indeed, the objective is to obtain coherent car trips without limiting the length of the activity chain to 3, as [4] did.

As seen in Figure 1, the kilometres travelled have to be defined after the *Activity Pattern* module. Three situations must be distinguished based on the trip's origin and destination. For trips which link home and work (*km H-W*), the approximate kilometres travelled, i.e. less than 1 km, 1-5 km and 5-10 km, is known from the *TUS (SD)*.

For all the other travels, except returning home, the *Travel duration* extracted from TUS data conditioned on the duration of the activity are sampled. Also, in this case, the travel activity was identified thanks to the place where the activity was carried out, i.e., the car. From another dataset publicly available provided by [24], i.e. *Speed* in Figure 1, the average speed at each hour for 225 European cities (plus other cities in all the continents) can be obtained. Thanks to it, the hourly average speeds are used to compute the approximate number of kilometres (*km* in Algorithm 1) covered every 10 minutes, considering as a first approximation a uniform motion.

For trips which link activities different from "Work" to "Home", the proposed solution considered the distance between the current position and home (*km back H* in Figure 1). However, since the travel for going back home is simply the distance between the current position and home, some behavioural rules of the agent need to be defined to model plausible journeys of the user. To this end, we introduce a spatial algorithm (Algorithm 1) to model the users' spatial behaviour and determine the place of activities that do not have a fixed location. In order to speed up the simulation of car trips on the map, a regular grid of approximately a 1 km square is created (the *Grid* block in Figure 1). The centroids of the map, i.e. the red dots in Figure 2, are used to find a plausible destination computing the Manhattan distance $L_1$ [25] among the centroid where the user is $C_{user}(x_{user}, y_{user})$

and all the others $C_n(x_n, y_n)$ as

$$L_1(C_{user}, C_n) = |x_{user} - x_n| + |y_{user} - y_n| \quad (5)$$

As depicted in Algorithm 1, the distance is in between the *km* computed ± a configurable tolerance (*tol*), we might have a plausible destination in that area (lines 1-7, 11-12). Otherwise, when the selected distance would bring the user outside the map, the maximum possible length of the travel is computed (lines 13-16 and 19-23). In this case, the remaining kilometres (i.e. the difference among *km* and the maximum distance) will be modelled as a search for the parking. In this case, the car will go back and forth between the last two nodes of the path.

If a plausible path inside the map can be found (line 25) and the trip's origin is not "Home", the algorithm determines how far the user is from home. Over a certain distance from home defined in the configurable distance *attract*, the next destination will have a higher probability between the previous location and home.

**Algorithm 1** User spatial behaviour

1: **procedure** INSIDEMAP($x$)
2: **for** $c$ *in centroids* **do**
3: $d\_uc = Manhattan\ distance\ user\ centroid\ to\ other\ centroid$
4: **if** $km - tol < d\_uc <= km + tol$ **then** $plausible\_centroids \leftarrow c$
5: **end if**
6: **end for**
7: **end procedure**
8: $origin,\ km,\ tol,\ attract \leftarrow inputs$
9: $GRID,\ MAP \leftarrow input\ from\ interaction\ with\ environment$
10: $plausible\_centroids,\ d\_ub,\ d\_ch \leftarrow [],\ [],\ []$
11: **if** $km < (map\ centre - boundary)$ **then** ▷ Inside the map
12: $plausible\_centroids = InsideMap(centroids)$
13: **else if** $km > size(MAP)$ **then**
14: $flag = 1$
15: $d\_ub \leftarrow Manhattan\ distances\ user\ to\ boundaries\ (centroids)$
16: $furthest = centroid\ with\ max(d\_ub)$
17: **else**
18: $plausible\_centroids = InsideMap(centroids)$
19: **if** $plausible\_centroids == 0$ **then**
20: $flag = 1$
21: $d\_ub \leftarrow Manhattan\ distances\ user\ to\ boundaries\ (centroids)$
22: $furthest = centroid\ with\ max(d\_ub)$
23: **end if**
24: **end if**
25: **if** flag != 1 **then**
26: $p \leftarrow []$
27: **if** $origin\ != \ "Home"$ **then**
28: $d\_uh \leftarrow Manhattan\ distance\ user\ to\ home\ centroid$
29: **if** $d\_uh > attract$ **then**
30: $distances = []$
31: **for** $c$ *in* $plausible\_centroids$ **do**
32: $d\_ch \leftarrow Manhattan\ distance\ centroid\ to\ home\ centroid$
33: **end for**
34: **for** $d$ *in* $distances$ **do** ▷ Centroids closer to home are more plausible
35: $scaled\ distances[c] = ((max(distances) - d) + min(distances)))$
36: **end for**
37: **for** $c$ *in* $plausible\_centroids$ **do**
38: $p[c] \leftarrow scaled\ distances[c]\ /\ sum(scaled\ distances)$
39: **end for**
40: **else**: ▷ Completely random
41: **for** $c$ *in* $plausible\_centroids$ **do**
42: $p[c] \leftarrow 1\ /\ number\ of\ plausible\ centroids$
43: **end for**
44: **end if**
45: **else**
46: **for** $c$ *in* $plausible\_centroids$ **do**
47: $p[c] \leftarrow 1\ /\ number\ of\ plausible\ centroids$
48: **end for**
49: **end if**
50: **end if**

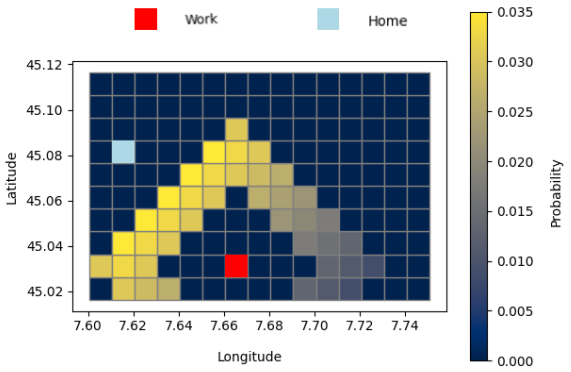


Fig. 3: Visual example of the selection of the next destination exploiting the generated *Grid* and the computed probability.

Figure 3 visualises the probability for the described case. The red square represents the area where the user was, while the light-blue square shows the area where the house of the user agent is located. Thus, the next destination will be picked according to the probability computed in lines 37-39. In the other cases, all the destinations are equally probable.

After determining the next destination, the algorithm computes the shortest path between the origin and the destination. For each segment of the chosen path, the length of the street and the maximum speed limit, i.e. the speed at which the user is supposed to travel, are known.
Thanks to the *Dummy traffic* module in Figure 1, the supposed user speed can be also decreased. As a first approximation, the difference between the maximum average speed and the average speed at that time read from the data of [24] is subtracted from the segment speed. Thus, the *Dummy traffic* module might not accurately capture real-time traffic fluctuations and congestion. However, it is considered to be precise enough for the purpose of the simulation.

The car movement could be simulated at a resolution lower than 10 minutes, knowing each street's maximum speed limit and length. The algorithm computes the average speed every 10 minutes to compare the obtained speed with the input data of [24]. Moreover, the user stops for a certain time at the stop sign and the traffic lights are considered. The amount of time is again configurable. Thus, the outputs from the *Path generator* in Figure 1 are i) the *Path* of the user, ii) the *Slope* and ii) the maximum *Speed* limit on each road. If the path includes very small segments - i.e. roads 15-30 metres long - these are aggregated with the following segment for simplicity.

### C. Driving behaviour of the User Agent

The *Path Generator* simulates the approximate behaviour of the user. Theoretically, the speed limit read from OSM on each road segment could be used directly. However, to better simulate the driver's behaviour, the acceleration and deceleration to obtain the desired speed for each segment, i.e., each road on the map, should be considered. To this end, the *Driving behaviour* module of the *User Agent* in Figure 1 is introduced.

As a first approximation, the travel on a segment has been considered composed of three periods: i) the acceleration

period, where the driver increases its speed with constant acceleration, i.e. uniformly accelerated motion; ii) the constant velocity period, i.e. uniform motion and iii) the deceleration period, i.e. uniformly decelerated motion. Notice that in the acceleration period, in the absence of traffic, the target speed equals the maximum allowed speed. Meanwhile, in the presence of traffic or when the segment is too short to reach the desired speed, it is lower than the maximum allowed speed.

However, no driver exhibits similar behaviour. Therefore, a random Gaussian noise with $\mu$ equal to zero and configurable $\sigma$ has been added to the uniform motion to account for the minor variations that occur on the straightaways due to the presence of other vehicles and lane changes.

It is important to emphasise that slightly different driving styles can be accounted for by playing with the Gaussian noise and increasing the target speed on certain roads for a subset of drivers, i.e. those who do not obey speed limits. Thus, the *Driving behaviour* model (see Section III-C) might also be seen as a synthetic driving patterns generator that might be used for different purposes.

The resulting curve can be filtered with a Savitzky-Golay filter [26], improving a signal trend's smoothness.

### D. EV charging strategy

The *EV charging strategy* module of Figure 1 implements the charging behaviour of the *User Agent*. Two main simple charging behaviours have been considered for modelling the decision to charge the EV: i) at home, i.e. the EV is always charged when the user is at home, and ii) when the SOC is below a particular configurable value. Therefore, one strategy is related to the parking place, and the other is related to the state of charge of the EV battery. Nevertheless, the framework can easily implement any other strategy. Indeed, more complex behaviours, e.g. behaviour under time-of-use tariffs or dynamic pricing scheme [27], could be tested thanks to the framework's modularity.

### E. EV model

The energy consumption of the EV is computed considering the specifics of the EV model and the modelled velocity for each road segment. The EV motion has been discretised over time in intervals of magnitude $\Delta$t equal to 0.1 seconds. Thus, at each time interval $k$, the acceleration $a$ is computed as

$$a_k = \frac{\Delta v}{\Delta t} \tag{6}$$

where $v$ is the velocity. As in [28], the tractive force is then

$$Ft_k = mgsin(\theta) + mgcos(\theta)c_{rr} + \frac{\rho A c_w}{2} v_k^2 + ma_k \tag{7}$$

where $\theta$ is the road slope, $m$ is the mass, $g$ is the gravity, $c_{rr}$ is the rolling resistance, $A$ is the frontal area, $\rho$ is the air density and $c_w$ is the aerodynamic coefficient of the EV under simulation. The *EV specification* inputs in Figure 1 specify the value of each coefficient.

The electrical power $P_{ele}$ is computed as

$$Pele_k = \frac{Ft_k \cdot v_k}{\eta} \tag{8}$$

where $\eta$ is the efficiency of the motor.

The corresponding discharge of the battery at each time interval is defined as follows:

$$SOC_k = SOC_{k-1} - \frac{Pele_k \cdot \Delta t}{C_{bat}} \tag{9}$$

where $C_{bat}$ is the nominal capacity of the battery.

For the sake of completeness, the EV battery recharges according to

$$SOC_{fin} = SOC_{ini} + \frac{P_{CS} \cdot t_{charge}}{C_{bat}} \tag{10}$$

where $SOC_{fin}$ and $SOC_{in}$ are the final and initial SOC in the considered time step, respectively, and $P_{CS}$ is the power received from the charging station.

## IV. Experimental results

To demonstrate the capability of the framework, two scenarios with a 1000 *User Agents* and 1000 *EV Agents* are analysed: i) *Scenario 1*, which analyses 30 weekdays and ii) *Scenario 2* that considers 30 weekends. TableIII summarises the input data of each block of Figure 1.

TABLE III: Input data of each block of Figure 1

| | Input data |
|---|---|
| TUS | The Italian TUS [29], considering only car drivers |
| OSM | The city of Turin |
| Speed | The average speed from [24] for the city of Turin |
| DTM | The DTM of Piedmont from [30] |
| EV specification | The same values of [28] |

Figure 2 illustrates the road network and the obtained *Grid*. The selected road network includes 11337 nodes and 17804 edges. Only trips inside the city, i.e. trips which last a maximum of 30 minutes when there is no traffic, are considered. Indeed, without traffic, drivers can cross the city in less than half an hour. Table IV lists the EV specifications for completeness. All EVs are equipped with a 40 kWh battery pack.

TABLE IV: Nissan Leaf Parameters from [28]

| Parameters | Value |
|---|---|
| EV mass $m$ | 1619 [kg] |
| Rolling resistance $c_{rr}$ | 0.01 |
| Air density $\rho$ | 1.28 [kg/m$^3$] |
| Frontal area $A$ | 2.576 [m$^2$] |
| Aerodynamic coefficient $c_w$ | 0.28 |

The two charging strategies are compared in both scenarios: i) drivers who charge their vehicle only at home or ii) always when the SOC is lower than 50%.

### A. EV usage and consumption aggregated results

The *Activity Pattern* module simulates the users' daily activities. Figure 4 depicts an example of the obtained user state proportions. The different use of time during weekdays (Figure 4a - *Scenario 1*) and weekends (Figure 4b - *Scenario 2*) is clearly visible. During weekdays (Figure 4a), many people

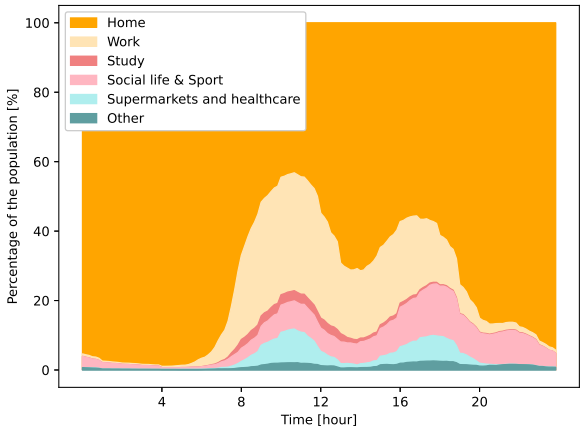


(a)

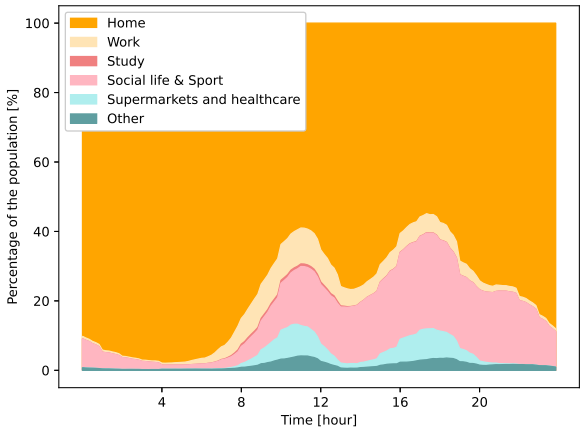


(b)

Fig. 4: Simulated user state proportions during 4a weekdays (*Scenario 1*) and 4b weekends (*Scenario 2*)

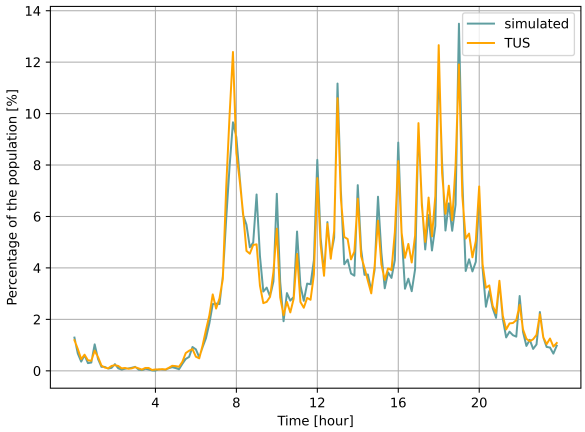


(a)

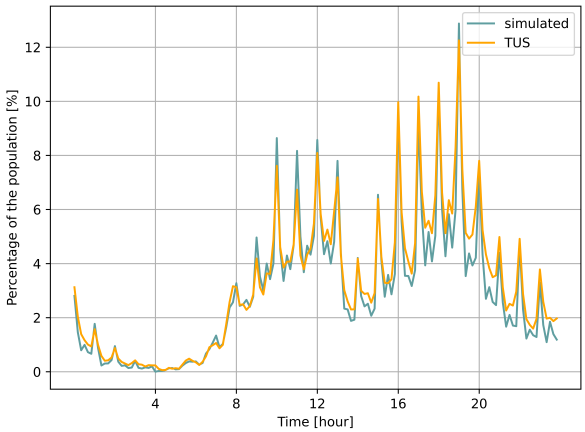


(b)

Fig. 5: Comparison of the simulated and TUS travel activity for 5a weekdays (*Scenario 1*) and 5b weekends (*Scenario 2*)

are engaged in work activities during daylight. Instead, during weekends (Figure 4b), the percentage of the activities coded as "Social life and Sport" increased with respect to weekdays. The "Study" activity represented only a minor percentage since only students who travelled by car were included in the analysis.

As described in SectionIII-A, the *Activity Pattern* generates only major activities. Therefore, to model the travel activity, it is necessary to use the *Path Generator*.

In Figure 5, the percentage of people driving every 10 minutes, i.e. the resolution of the TUS data, compared to the simulated ones, can be observed for both weekdays (Figure 5a - *Scenario 1*) and weekends (Figure 5b - *Scenario 2*). In Figure 5a, two significant spikes can be observed in the morning and the late afternoon, corresponding to the people going to work and home, respectively. A third spike is visible at lunchtime. Instead, during the weekend, travels concentrate in the late morning and the afternoon. In both cases, the simulated (blue curve) and the TUS (orange curve) data are remarkably similar.

To understand the goodness of the results, i) the Index of Agreement (IoA), i.e. the Willmott index; ii) the bias; iii) the Mean Absolute Error (MAE) and iv) the Root Mean Square Error (RMSE) are calculated. Table V summarises the results for both weekdays and weekends.

TABLE V: Comparison of model-produced estimates with TUS data

| | IoA | Bias [%] | MAE [%] | RMSE [%] |
|---|---|---|---|---|
| Weekdays | 0.988 | -0.097 | 0.408 | 0.615 |
| Weekends | 0.984 | -0.317 | 0.443 | 0.618 |

The IoA can assume values between 0 and 1, i.e. no agreement at all and a perfect match, respectively. Table V shows that the values of the IoA are pretty close to 1, i.e. higher than 0.98, on both weekdays and weekends. The simulation of the weekends shows a slightly larger bias with respect to the weekdays: -0.317 and -0.097, respectively. In both scenarios, the MAE and the RMSE are small, around 0.4 and 0.6, respectively. These results are not simply obtained from a sampling of the travel duration, as done in most of

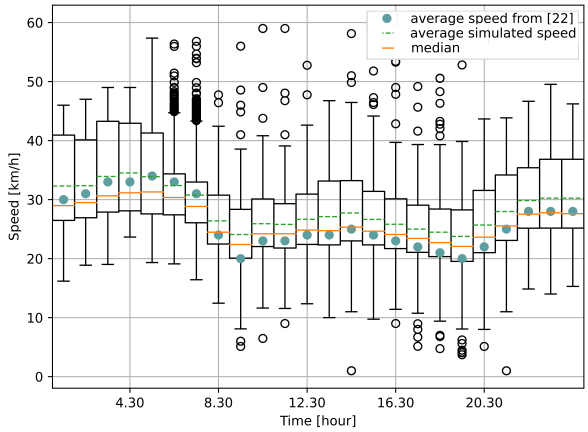


(a)

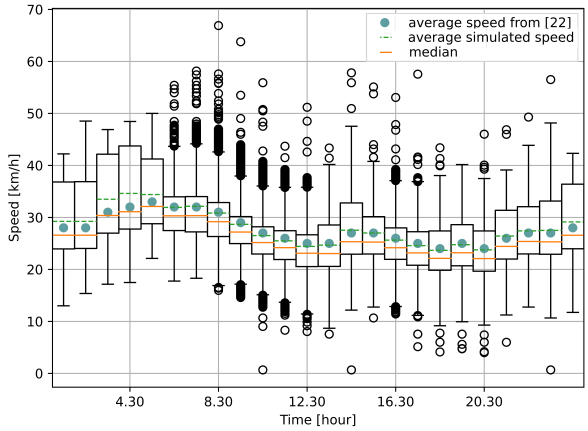


(b)

Fig. 6: Average simulated speed during 6a weekdays (*Scenario 1*) and during 6b weekends (*Scenario 2*) compared with [22]

the literature, but also from a user's behavioural model. The simulations show good results since the IoA is close to 1 and the errors are small.

Moreover, with the *Path Generator* we can also observe the average speed of the vehicle fleet every 10 minutes, as depicted in Figure 6. During the night, there is a greater spread with respect to the day. Very few cars are on the street at night, and the speed depends strongly on the shortest path chosen. During the day, the average speed decreases during high peak traffic. It is worth highlighting that using the speed limit retrieved from OSM, the simulated speed does not perfectly match the data collected in [24], especially when simulating weekdays. Indeed, in Table VI, the IoA of weekdays is 0.898, and the simulated speed is higher than the one observed in [24], with a bias around 2.7 km/h. The weekends instead show low errors. In any case, the simulated speed is realistic, and the error rates reported in Table VI are negligible.

Overall, the results demonstrate that the *Activity Pattern* and the *Path Generator* modules are able to replicate activities and vehicle usage.

Figure 7 compares both scenarios' monthly average power withdrawal results. At the beginning of the simulation, it was supposed that the EVs were fully charged; therefore, the batteries were not charged in the first days of the simulation.

TABLE VI: Comparison of model-produced estimates with data from [24]

| | IoA | Bias [km/h] | MAE [km/h] | RMSE [km/h] |
|---|---|---|---|---|
| Weekdays | 0.898 | 2.272 | 2.354 | 2.581 |
| Weekends | 0.974 | 0.334 | 0.676 | 0.955 |

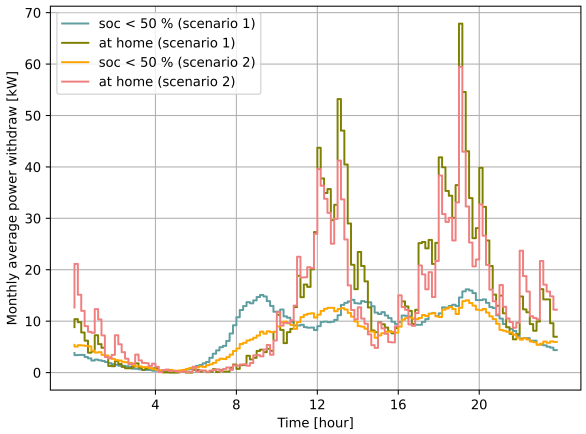


Fig. 7: Monthly average power withdrawal comparison

On both weekdays (blue curve) and weekends (orange curve), the strategy of charging the EV when the SOC is below 50% shows better results than the strategy of always charging the EV when at home. Indeed, in the former case, the curve is rather flat. Only two and three minor bumps can be noticed in the orange and blue curves, respectively. Comparing Figure 7 with Figure 5a and Figure 5b, it is possible to understand that this increase always follows the traffic peaks. The green and the pink curves show the electricity load for the charging strategy at home for weekends and weekdays, respectively. With this strategy, the peaks happen at similar times. If charging stations are available only at user premises and the users get used to charging the EV as soon as they get home, problems might arise because of the high electricity demand. In all scenarios, few EVs charge at night since urban trips are quite short; thus, EVs are already charged before dawn.

### B. *Single user's Path Generator and Driving behaviour results*

After showing the aggregated results, a detailed output of the *Path Generator*, i.e. i) Path, ii) Slope, iii) Target speed, i.e. the speed limit also considering the traffic, of a *User Agent* single trip from its workplace in the city centre to its home on the hillside is illustrated. Figure 8 shows the travel route.

The altitude obtained from the DTM, the computed slope and the target speed are shown in Figure 9. It should be noticed that the speed can be an average of more than one segment as described in Section III-B. Moreover, the presence of traffic was considered. In particular, the targeted speed was 10 km

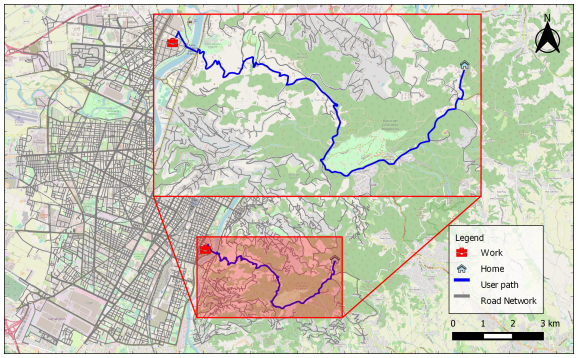


Fig. 8: Shortest path found on the map between work, i.e. the origin, and home, i.e. the destination

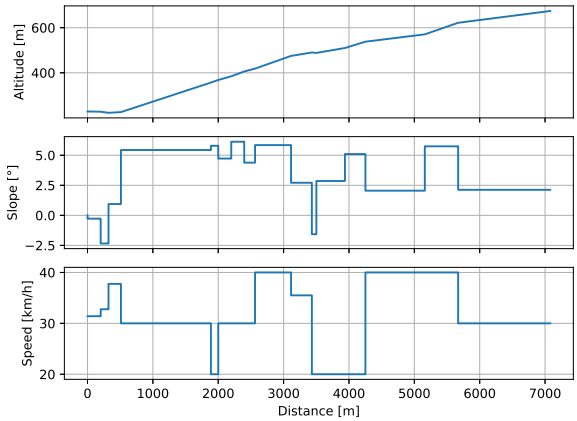


Fig. 9: Altitude, slope and target speed for the selected path

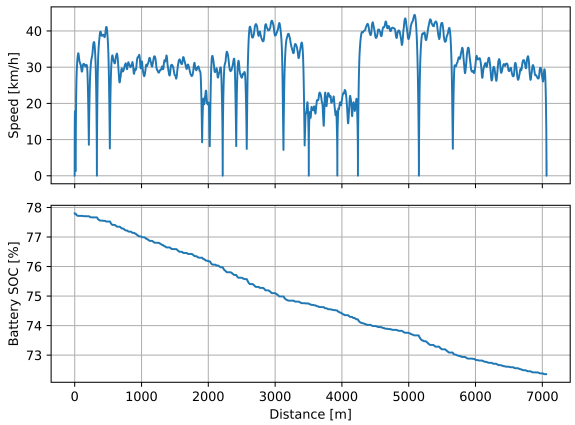


Fig. 10: *Driver behaviour* output example

less than the usual speed signal. Therefore, while the road sign indicates a speed limit between 30 km/h and 50 km/h, the target speed of the user is between 20 km/h and 40 km/h.

The corresponding *Driving Behaviour* is depicted in Figure 10. For each road segment, it is not known if a user stops or only decreases its velocity. Therefore, its behaviour is computed randomly.

For completeness, the EV battery's SOC is also given in Figure 10, where the SOC goes from around 78% to 72% with a total energy consumption of 2.17 kWh. Notice that with a constant slope of 1 degree, the total energy consumption would be 1.27 kWh. A more detailed analysis of the *EV model*'s results will be better discussed in the following scenario with a comparison with real data.

### C. Driving behaviour and EV consumption comparison

*Scenario 1* and *Scenario 2* were compared with TUS data and average speeds [24] showing good results. Moreover, hypothetical future charging scenarios were discussed in detail in an aggregated form. Detailed results for a single user were provided. However, the *Driving behaviour* module and the *EV model* were not validated because driving patterns and the corresponding EV consumption data are seldom available. Figure 11 (orange curve) replicates EV data presented in [28] collected from an actual vehicle to perform a qualitative comparison with real measurements.

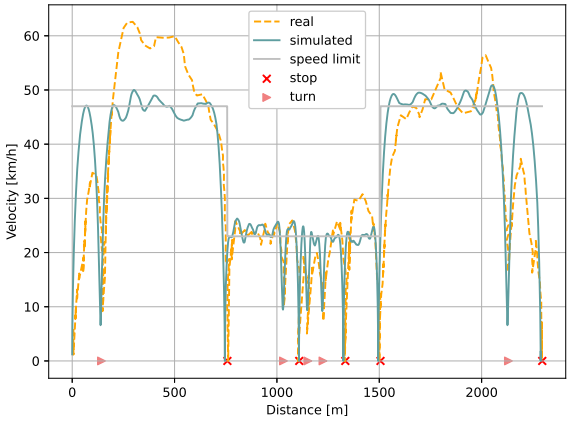


Fig. 11: Comparison of simulated and real velocity from [28]

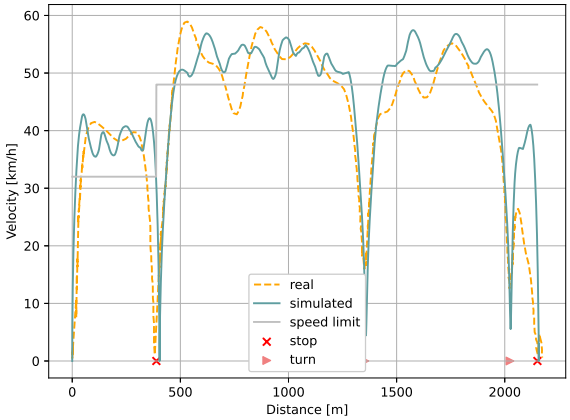


Fig. 12: Comparison of simulated and real velocity from [28]

Given the input of the speed limit for each street (grey curve), i.e. the speed that the EV is supposed to travel at, to the driving behaviour sub-module, the blue curve is obtained. Notably, the real data and the data generated artificially show similar trends. The pink arrows highlight when the vehicle turns, corresponding to a decrease in speed, while the red

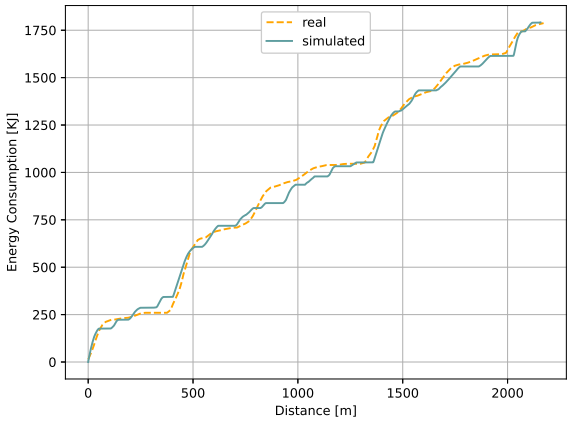


Fig. 13: Comparison between simulated and real EV consumption taken from [28]

cross indicates where the vehicle stops. In this simulation, the stops and turns are known as a priori and are not computed randomly, as in the previous scenarios. In Figure 11, the real and the simulated velocities are different in the first segments since the real driver did not respect the speed limit. Anyhow, it would be possible to obtain similar behaviour by including the behaviour of a driver who sometimes does not respect the speed limit. For example, in Figure 12 the user exceeded the speed limit, i.e. the target speed is 5 km/h higher than the speed limit.

Figure 13 plots the corresponding battery consumption in the function of the distance. The orange curve represents the actual energy consumption data from [28] while the blue curve is the output of the *EV model* of Figure 1 and the same values of [28] for the *EV specification*, see Table IV. The two curves show similar trends.

## V. Conclusion

The increasing sale of EVs requires new tools capable of realistically modelling the behaviour of users, their trips and their EV consumption. Unfortunately, city-specific data are seldom available. Thus, state-of-the-art methodologies are usually based on travel surveys. However, the latter are also only available in some countries. Furthermore, there is a lack of standardised data-based methodologies that can be used without more precise data.

To this end, we propose a new framework to simulate the travel activities of a population of agents with heterogeneous characteristics, starting from almost worldwide available data, i.e. TUS. Urban trips are modelled thanks to a specific road network of the city under study, characterised by different speed limits and driving behaviours. Then, EV consumption is computed. Thus, the proposed methodology allows us to estimate EV consumption in the urban context starting from limited data, allowing specific studies in all major cities and comparing different charging strategies. However, the proposed methodology would necessitate modifications for rural or intercity travel patterns. This issue will be addressed in the future.

The modularity of the framework allowed us to test different modules easily. The *Activity Pattern* module and the travel activity were validated, showing promising results. The *Driving behaviour* and *EV model* modules were qualitatively compared to real data, demonstrating that the model can generate plausible driver behaviours and corresponding EV consumption, potentially offering the opportunity to use the modules for different purposes. Having access to more variable real data would allow researchers to understand if, for example, the *Driving behaviour* module is realistic enough to generate synthetic driving patterns. If not, it could be improved considering all sources of uncertainties, interactions among cars, road boundaries and line lanes as done in [31]. Moreover, OSM might also be substituted with a more precise and up-to-date road network [32] thanks to the framework's modularity which enables substituting one single module of Figure 1 without affecting the rest of the framework.

Future massive EV diffusion can make the power system unstable, requiring the testing of new Demand-Side Management programs that consider i) EV characteristics, ii) user willingness and iii) the grid state [33]. The presented agent-based framework somehow enables us to model the first two points, while thanks to co-simulation, the grid can be included in the simulation in future. Indeed, EVs-grid interactions would allow the framework's user to test algorithms to manage the EV charging process as done in [34], where the waiting time before the plugin is minimised and grid stability is preserved, or that consider the bidirectional power flow between the EV and the grid, e.g. [35]. Other aspects could be analysed, such as road traffic $CO_2$ emissions with advanced models, e.g. [36], or the inclusion of electric public transport models and related strategies [37].

To conclude, the proposed framework enables the modelling of EV mobility in multiple countries, eliminating the reliance on travel-specific data and providing the basis for future more complex scenarios.

## References

[1] UNFCCC_Authors, "Decision /CP.26 Glasgow Climate Pact," 2021, [2022-02-01]. [Online]. Available: https://unfccc.int/sites/default/files/resource/cop26_auv_2f_cover_decision.pdf

[2] E. Commission, "Zero emission vehicles: first 'fit for 55' deal will end the sale of new co2 emitting cars in europe by 2035," 2022, (accessed: 28.03.2023). [Online]. Available: https://ec.europa.eu/commission/presscorner/detail/en/ip_22_6462

[3] I. C. Network, "Postponement of the vote on stopping endothermic engines from 2035," 2024, (accessed: 19.05.2024). [Online]. Available: https://www.italiaclima.org/en/postponement-of-the-vote-on-stopping-endothermic-engines-from-2035/

[4] Y. Xiang, Z. Jiang, C. Gu, F. Teng, X. Wei, and Y. Wang, "Electric vehicle charging in smart grid: A spatial-temporal simulation method," *Energy*, vol. 189, p. 116221, 2019.

[5] G. Pareschi, L. Küng, G. Georges, and K. Boulouchos, "Are travel surveys a good basis for ev models? validation of simulated charging profiles against empirical data," *Appl. Energy*, vol. 275, p. 115318, 2020.

[6] M. Iqbal, L. Kütt, M. Lehtonen, R. J. Millar, V. Püvi, A. Rassõlkin, and G. L. Demidova, "Travel activity based stochastic modelling of load and charging state of electric vehicles," *Sustainability*, vol. 13, no. 3, 2021.

[7] Y. Wang and D. Infield, "Markov chain monte carlo simulation of electric vehicle use for network integration studies," *International Journal of Electrical Power & Energy Systems*, vol. 99, pp. 85–94, 2018.

[8] J. Zhang, J. Yan, Y. Liu, H. Zhang, and G. Lv, "Daily electric vehicle charging load profiles considering demographics of vehicle users," *Applied Energy*, vol. 274, p. 115063, 2020.

[9] D. Fischer, A. Harbrecht, A. Surmann, and R. McKenna, "Electric vehicles' impacts on residential electric local profiles – a stochastic modelling approach considering socio-economic, behavioural and spatial factors," *Applied Energy*, vol. 233-234, pp. 644–658, 2019.

[10] A. AHERN, G. WEYMAN, M. REDELBACH, A. SCHULZ, L. AKKERMANS, L. VANNACCI, E. ANOYRKATI, G. A. VON *et al.*, "Analysis of national travel statistics in europe optimism wp2: harmonisation of national travel statistics in europe," 2013.

[11] E. Commission and Eurostat, *Harmonised European Time Use Surveys : 2018 guidelines*. Publications Office, 2019.

[12] L. Bottaccioli, S. Di Cataldo, A. Acquaviva, and E. Patti, "Realistic multi-scale modeling of household electricity behaviors," *IEEE Access*, vol. 7, pp. 2467–2489, 2019.

[13] J. Rolink and C. Rehtanz, "Large-scale modeling of grid-connected electric vehicles," *IEEE Transactions on Power Delivery*, vol. 28, no. 2, pp. 894–902, 2013.

[14] S. Scherfke. aiomas' documentation. [Accessed: 2019-01-10]. [Online]. Available: https://aiomas.readthedocs.io/en/latest/

[15] M. Shepero and J. Munkhammar, "Spatial markov chain model for electric vehicle charging in cities using geographical information system (gis) data," *Applied Energy*, vol. 231, pp. 1089–1099, 2018.

[16] C. Marmaras, E. Xydas, and L. Cipcigan, "Simulation of electric vehicle driver behaviour in road transport and electric power networks," *Transportation Research Part C: Emerging Technologies*, vol. 80, pp. 239–256, 2017. [Online]. Available: https://www.sciencedirect.com/science/article/pii/S0968090X17301341

[17] S. Torres, O. Barambones, J. M. Gonzalez de Durana, F. Marzabal, E. Kremers, and J. Wirges, "Agent-based modelling of electric vehicle driving and charging behavior," in *In Proc of 2015 23rd MED*, 2015, pp. 459–464.

[18] R. Wolbertus, R. van den Hoed, M. Kroesen, and C. Chorus, "Charging infrastructure roll-out strategies for large scale introduction of electric vehicles in urban areas: An agent-based simulation study," *Transportation Research Part A: Policy and Practice*, vol. 148, pp. 262–285, 2021.

[19] A. Gil Solá and B. Vilhelmson, "To choose, or not to choose, a nearby activity option: Understanding the gendered role of proximity in urban settings," *Journal of Transport Geography*, vol. 99, p. 103301, 2022.

[20] P. Brémaud, *Markov chains: Gibbs fields, Monte Carlo simulation, and queues*. Springer Science & Business Media, 2001, vol. 31.

[21] J. Jacques and M. Raimondo, *Semi-Markov risk models for finance, insurance and reliability*. Springer, 2007.

[22] M. M. Giovanni Masala, Giuseppina Cannas, "Survival probabilities for hiv infected patients through semi-markov processes," *Biometrical Letters*, vol. 51, no. 1, pp. 13–36, 2014.

[23] OSM, "Openstreetmap," 2010, [2020-11-15]. [Online]. Available: https://www.openstreetmap.org/about

[24] TomTom, "Turin traffic," 2023, (accessed: 13.03.2023). [Online]. Available: https://www.tomtom.com/traffic-index/turin-traffic/

[25] F. E. Szabo, "M," in *The Linear Algebra Survival Guide*, F. E. Szabo, Ed. Boston: Academic Press, 2015, pp. 219–233.

[26] R. W. Schafer, "What is a savitzky-golay filter? [lecture notes]," *IEEE Signal Processing Magazine*, vol. 28, no. 4, pp. 111–117, 2011.

[27] C. Fang, H. Lu, Y. Hong, S. Liu, and J. Chang, "Dynamic pricing for electric vehicle extreme fast charging," *IEEE Transactions on Intelligent Transportation Systems*, vol. 22, no. 1, pp. 531–541, 2021.

[28] H. Shen, Z. Wang, X. Zhou, M. Lamantia, K. Yang, P. Chen, and J. Wang, "Electric vehicle velocity and energy consumption predictions using transformer and markov-chain monte carlo," *IEEE Transactions on Transportation Electrification*, vol. 8, no. 3, pp. 3836–3847, 2022.

[29] I. N. di Statistica, "Multipurpose survey on households: Time use - microdata for research purposes," 2013, (accessed: 09.12.2022). [Online]. Available: https://www.istat.it/en/archivio/202524

[30] R. Piemonte, "Ripresa aerea ice 2009-2011 - dtm 25," 2011, (accessed: 08.12.2022). [Online]. Available: https://www.geoportale.piemonte.it/geonetwork/srv/api/records/r_piemon:f4b00ea3-6e98-4a04-a2ae-bc5d4f285aed

[31] X. Liu, Y. Wang, K. Jiang, Z. Zhou, K. Nam, and C. Yin, "Interactive trajectory prediction using a driving risk map-integrated deep learning method for surrounding vehicles on highways," *IEEE Transactions on Intelligent Transportation Systems*, vol. 23, no. 10, pp. 19 076–19 087, 2022.

[32] Z. Li, Y. Wang, R. Zhang, F. Ding, C. Wei, and J.-G. Lu, "A lidar-openstreetmap matching method for vehicle global position initialization based on boundary directional feature extraction," *IEEE Transactions on Intelligent Vehicles*, pp. 1–13, 2024.

[33] D. Said, "A survey on information communication technologies in modern demand-side management for smart grids: Challenges, solutions, and opportunities," *IEEE Engineering Management Review*, vol. 51, no. 1, pp. 76–107, 2023.

[34] D. Said, S. Cherkaoui, and L. Khoukhi, "Guidance model for ev charging service," in *2015 IEEE International Conference on Communications (ICC)*, 2015, pp. 5765–5770.

[35] D. Said and H. T. Mouftah, "A novel electric vehicles charging/discharging management protocol based on queuing model," *IEEE Transactions on Intelligent Vehicles*, vol. 5, no. 1, pp. 100–111, 2020.

[36] B. Liu, F. Li, Y. Hou, S. Antonio Biancardo, and X. Ma, "Unveiling built environment impacts on traffic co2 emissions using geo-cnn weighted regression," *Transportation Research Part D: Transport and Environment*, vol. 132, p. 104266, 2024. [Online]. Available: https://www.sciencedirect.com/science/article/pii/S1361920924002232

[37] X. Liu, W.-L. Shang, G. H. de Almeida Correia, Z. Liu, and X. Ma, "A sustainable battery scheduling and echelon utilization framework for electric bus network with photovoltaic charging infrastructure," *Sustainable Cities and Society*, vol. 101, p. 105108, 2024. [Online]. Available: https://www.sciencedirect.com/science/article/pii/S2210670723007175